Int. J. Solids Structures Vol. 30, No. 6, pp. 797–823, 1993
Printed in Great Britain

0020–7683/93 $6.00+.00

DYNAMIC ANALYSIS OF COMPOSITE MEMBERS WITH INTERLAYER SLIP

ULF ARNE GIRHAMMAR† and DANHUA PAN
Royal Institute of Technology (KTH), S-100 44 Stockholm, Sweden

(*Received* 26 *September* 1991; *in revised form* 8 *October* 1992)

Abstract—The exact and approximate analysis of composite members with partial interaction and subjected to general dynamic loading are presented. General closed-form solutions for the displacement functions and the various internal actions in the composite elements are presented for both the exact and approximate cases. The solutions reduce to the well-known values for the extreme cases of interlayer connection: non-composite and full composite action, respectively. An approximate solution for the eigenfrequencies in the exact analysis procedure is proposed and evaluated by comparison with the exact solution. These solutions show the effect of interlayer connection on the eigenfrequency. The exact and approximate analysis procedures are applied to simply-supported beams subjected to impulsive and step loadings to illustrate the difference in the solutions obtained by the two procedures. Very good agreement is obtained between the results of exact and approximate analysis of these particular cases.

1. INTRODUCTION

Composite structures of different materials are frequently used in building, bridge and shelter construction (Fig. 1). Those structures can be subject to different kinds of dynamic loadings. Buildings are subjected to wind and gust loadings, and machine and human loads, bridges to traffic and moving loads, and shelters to blast, ground shock wave and impact loadings.

Composite structures are defined as structures built up by structural self-carrying subelements connected by shear connectors to form an interacting unit (Fig. 1). The behaviour of composite members depends to a large degree on the type of connection between the subcomponents. In the case of dynamic loading the shear connectors also govern the energy absorption capacity and the damping characteristics. A typical load-slip diagram for a flexible shear connection is shown in Fig. 2. The usual non-linear relationship is frequently approximated by a linear relationship, $V_s = K\Delta u$, i.e. by using a constant slip modulus (K). For members subject to static loads the secant slip modulus is frequently used (dashed line in Fig. 2), but in the case of dynamic and buckling loads, the tangent slip modulus should be used (dashed-dotted line in Fig. 2). The concentrated forces from mechanical shear connectors are usually distributed uniformly along the length of the member in order to simplify the analysis.

Exact static analysis procedure for composite beams with partial interaction is well established. Corresponding exact analysis procedure for beam-columns has been presented by Girhammar and Gopu (1991, 1993a). Also, approximate static analysis procedures have been proposed by Girhammar (1992) for composite beams and by Girhammar and Gopu (1991, 1993b) for beam-columns. The purpose of this paper is to present corresponding exact and approximate dynamic analysis procedures for free and forced vibrations of composite Euler–Bernoulli beams with interlayer slip. The dynamic analyses of composite beams carried out by Girhammar (1985a) for a simple case and by Girhammar and Pan (1992) form the basis of this work. Henghold (1972) derived and solved the governing differential

† Current address: Swedish University of Agricultural Sciences (SLU), Department of Farm Buildings (LBT), Box 7032, S-750 07 Uppsala, Sweden.

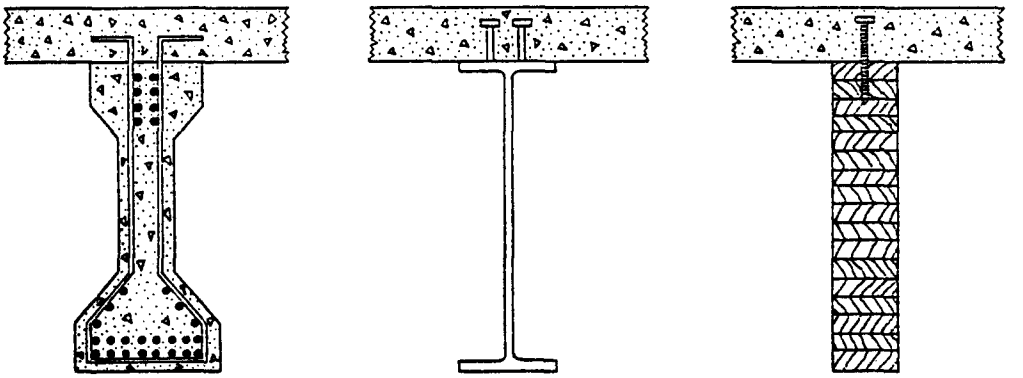

Fig. 1. Typical composite structures of concrete, steel and wood used in bridge, building and shelter construction.

equations for free vibrations of layered beams including slip. The exact analysis is based on the one-dimensional, linear elastic, partial composite action theory, and the approximate analysis on energy considerations for an equivalent single-degree of freedom system. Full composite action (infinite slip stiffness, $K \to \infty$) and non-composite action (zero slip stiffness, $K \to 0$) represent upper and lower bounds for the partial composite action.

2. EXACT STATIC ANALYSIS

The exact dynamic analysis procedure developed in the next section will be based on the exact static analysis procedure presented in this section (Girhammar and Gopu, 1993a). The geometric parameters defining a typical composite beam with two subelements of different materials are shown in Fig. 3. A general loading on a typical beam is shown in Fig. 4. The lateral load is distributed with an intensity q which varies with the distance x along the beam. The x-axis of the coordinate system is located in the centroid of the fully composite section. The support conditions are not specified, since they can be of any kind. Only the location of supports is represented by dots as in Fig. 4.

Consider the free-body diagram of a differential element (Fig. 5) in the composite beam subject to transverse load as shown. Moment, shear force, normal force and slip force per unit length are denoted as M, V, N and V_s, respectively. The aforementioned one-dimensional, linear elastic, partial-composite-action theory for a composite beam is based on the assumptions given by Girhammar and Gopu (1993a) with the additional assumptions

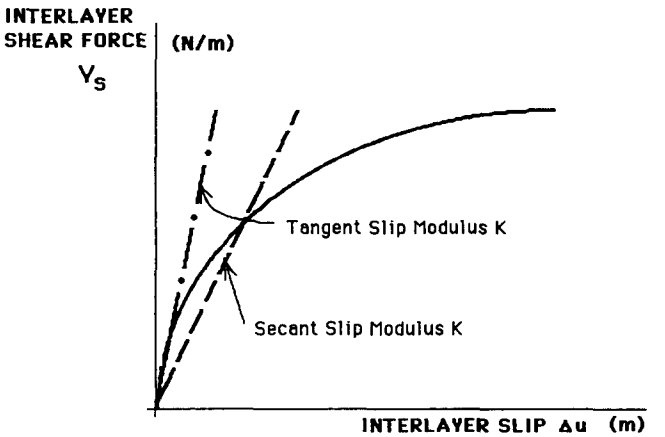

Fig. 2. Typical load-slip characteristics for flexible shear connectors in composite structures.

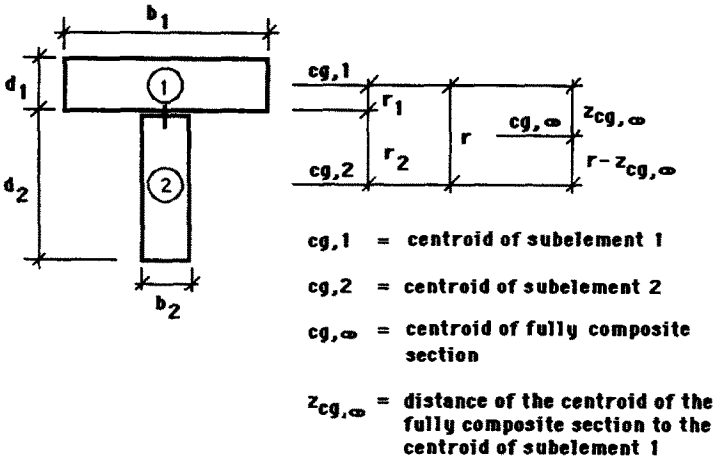

Fig. 3. Geometric parameters of composite beam.

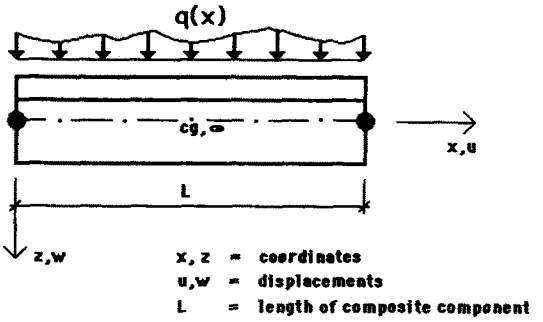

Fig. 4. Loads acting on and coordinate system for a composite beam.

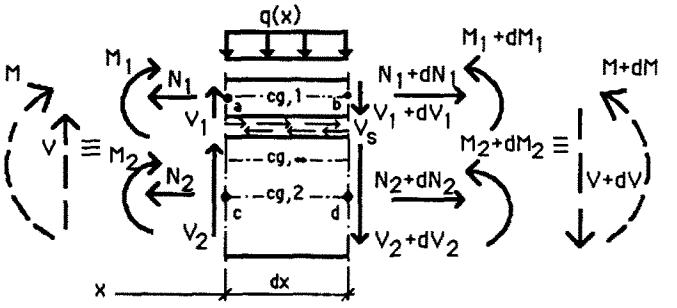

Fig. 5. Differential element in the composite beam subject to a distributed transverse load.

that friction effects and damping are neglected. They derived the following differential equation in terms of the displacement w (in the case of no axial forces):

$$\frac{d^4w}{dx^4} - \alpha^2 \frac{d^2w}{dx^2} = \alpha^2 \frac{M}{EI_\infty} - \frac{1}{EI_0} \frac{d^2M}{dx^2} \tag{1a}$$

or

$$\frac{d^6w}{dx^6} - \alpha^2 \frac{d^4w}{dx^4} = -\alpha^2 \frac{q}{EI_\infty} + \frac{1}{EI_0} \frac{d^2q}{dx^2}, \tag{1b}$$

where

$$\alpha^2 = \frac{Kr^2}{EI_0\left(1 - \frac{EI_0}{EI_\infty}\right)}, \tag{2}$$

$$\beta = \frac{Kr}{EI_0}, \tag{3}$$

$$EI_0 = E_1I_1 + E_2I_2, \tag{4}$$

$$EI_\infty = \frac{EI_0}{1 - \frac{\beta r}{\alpha^2}} = EI_0 + \frac{EA_p r^2}{EA_0}, \tag{5}$$

$$EA_0 = E_1A_1 + E_2A_2, \tag{6}$$

$$EA_p = E_1A_1 \cdot E_2A_2, \tag{7}$$

and K = slip modulus (N m^{-2}), E_iI_i = bending stiffness of the ith subelement, EI_0 = bending stiffness of the non-composite section ($K \to 0$), EI_∞ = bending stiffness of the fully composite section ($K \to \infty$), E_iA_i = axial stiffness of the ith subelement, EA_0, EA_p = sum and product, respectively, of the axial stiffness of subelements, r = distance between the two centroids.

The general solution of eqn (1b) is given by (Girhammar and Gopu, 1993a):

$$w = a_1 \sinh(\alpha x) + a_2 \cosh(\alpha x) + a_3x^3 + a_4x^2 + a_5x + a_6 + w_{ps}, \tag{8}$$

where a_1–a_6 are integration constants determined by the boundary conditions and

$$w_{ps} = \frac{1}{\alpha^5 EI_0} \int_0^x \left\{\alpha^2 \frac{EI_0}{EI_\infty} q(s) - \frac{d^2q(s)}{ds^2}\right\} \left\{\alpha(x-s) + \frac{\alpha^3}{6}(x-s)^3 - \sinh[\alpha(x-s)]\right\} ds, \tag{9}$$

where s is a dummy variable. Knowing the solution w for a given set of boundary conditions, the various internal actions can be given in terms of w as follows (Girhammar and Gopu, 1993a):

$$M = M_1 + M_2 - N_1r = \frac{EI_\infty}{\alpha^2} \frac{d^4w}{dx^4} - EI_\infty \frac{d^2w}{dx^2} - \frac{EI_\infty}{\alpha^2 EI_0} q, \tag{10}$$

$$V = V_1 + V_2 = \frac{dM}{dx}, \tag{11}$$

$$N_1 = -N_2 = -\frac{1}{r}\left(M + EI_0 \frac{d^2w}{dx^2}\right), \tag{12}$$

$$V_s = K\Delta u = -\frac{dN_1}{dx} = \frac{dN_2}{dx}, \tag{13}$$

$$M_i = -E_i I_i \frac{d^2 w}{dx^2}, \tag{14}$$

$$V_i = \frac{dM_i}{dx} + V_s r_i. \tag{15}$$

The boundary conditions can be expressed as follows: for a *pinned end* the conditions $w = M_i = N_1 = 0$ give, according to eqns (14) and (12):

$$w = 0,$$
$$\frac{d^2 w}{dx^2} = 0,$$
$$\frac{d^4 w}{dx^4} = \frac{q}{EI_0}. \tag{16a,b,c}$$

For a *clamped end* the conditions $w = dw/dx = \Delta u = 0$ give, according to eqn (13):

$$w = 0,$$
$$\frac{dw}{dx} = 0,$$
$$\frac{d^5 w}{dx^5} - \alpha^2 \left(1 - \frac{EI_0}{EI_\infty}\right) \frac{d^3 w}{dx^3} = \frac{1}{EI_0} \frac{dq}{dx}. \tag{17a,b,c}$$

For a *free end* the conditions $M_i = N_1 = V = 0$ give, according to eqns (14), (12) and (11):

$$\frac{d^2 w}{dx^2} = 0,$$
$$\frac{d^4 w}{dx^4} = \frac{q}{EI_0},$$
$$\frac{d^5 w}{dx^5} - \alpha^2 \frac{d^3 w}{dx^3} = \frac{1}{EI_0} \frac{dq}{dx}. \tag{18a,b,c}$$

It can be shown by the use of the principle of minimum energy that the differential equation (1b) together with the boundary conditions (16), (17) and/or (18) constitutes a well-posed problem.

3. EXACT DYNAMIC ANALYSIS

3.1. *General*

In the case of dynamic loading, $p(x, t)$, the following relationship is valid according to d'Alembert's principle:

$$q = -\frac{\partial^2 M}{\partial x^2} = -m \frac{\partial^2 w}{\partial t^2} + p, \tag{19}$$

where $m = m_1 + m_2$ [kg m^{-1}] is the sum of the mass per unit length of each subelement. Substituting eqn (19) in eqn (1b), the governing partial differential equation for composite members with incomplete interaction subject to dynamic loading, $p(x, t)$, is given as

$$\frac{\partial^6 w}{\partial x^6} - \alpha^2 \frac{\partial^4 w}{\partial x^4} + \frac{m}{EI_0} \frac{\partial^4 w}{\partial t^2 \partial x^2} - \alpha^2 \frac{m}{EI_\infty} \frac{\partial^2 w}{\partial t^2} = -\frac{\alpha^2}{EI_\infty} p + \frac{1}{EI_0} \frac{\partial^2 p}{\partial x^2}. \tag{20}$$

The general solution for eqn (20) can, according to the method of separation of variables, be written as

$$w = \phi(x) f(t) = \sum_n \phi_n(x) f_n(t); \quad \text{free vibrations } (p = 0), \tag{21}$$

$$w = \phi(x) F(t) = \sum_n \phi_n(x) F_n(t); \quad \text{forced vibrations } (p = p(x, t)), \tag{22}$$

where ϕ_n are the eigenmodes determined for $p = 0$ and depend on the boundary conditions, f_n are the time functions for natural vibrations, and F_n are the time functions determined for $p = p(x, t)$ and depend on the initial conditions. If the solution for w is known, the internal moment is given by substituting eqn (19) into eqn (10), i.e.

$$M = M_1 + M_2 - N_1 r = \frac{EI_\infty}{\alpha^2} \frac{\partial^4 w}{\partial x^4} - EI_\infty \frac{\partial^2 w}{\partial x^2} + \frac{m}{\alpha^2} \frac{EI_\infty}{EI_0} \frac{\partial^2 w}{\partial t^2} - \frac{EI_\infty}{\alpha^2 EI_0} p. \tag{23}$$

The other internal actions are then obtained from eqns (11)–(15) recognizing that the internal moment now is given by eqn (23) and that differentiation with respect to x now represents partial differentiation with respect to x. For the special case of *non-composite action* ($V_s = 0$; $K \to 0$), the internal actions can be computed from eqns (12)–(15) recognizing eqn (23) and that $\partial^2 w/\partial x^2 = -M/EI_0$ and $\partial^3 w/\partial x^3 = -V/EI_0$:

$$N_{1,0} = -N_{2,0} = 0, \tag{24}$$

$$V_{s,0} = 0, \tag{25}$$

$$M_{i,0} = \frac{E_i I_i}{EI_0} M, \tag{26}$$

$$V_{i,0} = \frac{E_i I_i}{EI_0} V + V_{s,0} r_i, \tag{27}$$

where the second subscript 0 implies solutions corresponding to non-composite action. For the other special limit case of *fully composite action* ($\Delta u = 0$; $K \to \infty$), the internal actions can be obtained from eqns (12)–(15) after recognizing eqn (23) and that $\partial^2 w/\partial x^2 = -M/EI_\infty$ and $\partial^3 w/\partial x^3 = -V/EI_\infty$:

$$N_{1,\infty} = -N_{2,\infty} = \left(1 - \frac{EI_0}{EI_\infty}\right) \frac{M}{r}, \tag{28}$$

$$V_{s,\infty} = -\left(1 - \frac{EI_0}{EI_\infty}\right) \frac{V}{r}, \tag{29}$$

$$M_{i,\infty} = \frac{E_i I_i}{EI_\infty} M, \tag{30}$$

$$V_{i,\infty} = \frac{E_i I_i}{EI_\infty} V + V_{s,\infty} r_i, \tag{31}$$

where the second subscript ∞ implies solutions corresponding to full composite action.

The boundary conditions can be obtained by substituting eqn (19) into eqns (16)–(18). The boundary conditions for *pinned and clamped ends* are obtained from eqns (16) and (17), respectively, changing $\mathrm{d}/\mathrm{d}x \to \partial/\partial x$ and $q \to p$. For a *free end* the expressions are obtained as:

$$\frac{\partial^2 w}{\partial x^2} = 0,$$

$$\frac{\partial^4 w}{\partial x^4} + \frac{m}{EI_0}\frac{\partial^2 w}{\partial t^2} = \frac{p}{EI_0},$$

$$\frac{\partial^5 w}{\partial x^5} - \alpha^2 \frac{\partial^3 w}{\partial x^3} + \frac{m}{EI_0}\frac{\partial^3 w}{\partial x\,\partial t^2} = \frac{1}{EI_0}\frac{\partial p}{\partial x}. \tag{32a,b,c}$$

The initial conditions are expressed in the conventional way by the initial displacement $w(x, 0)$ and by the initial velocity $\partial w(x, 0)/\partial t$.

3.2. *Free vibrations*

Introducing expression (21) in (20) for $p = 0$ the following two ordinary differential equations are obtained:

$$\frac{\mathrm{d}^6\phi_n}{\mathrm{d}x^6} - \alpha^2\frac{\mathrm{d}^4\phi_n}{\mathrm{d}x^4} - \omega_n^2\frac{m}{EI_0}\frac{\mathrm{d}^2\phi_n}{\mathrm{d}x^2} + \omega_n^2\alpha^2\frac{m}{EI_\infty}\phi_n = 0, \tag{33}$$

$$\frac{\mathrm{d}^2 f_n}{\mathrm{d}t^2} + \omega_n^2 f_n = 0. \tag{34}$$

Equations (33) and (34) imply that the common constant for the two equations, the eigenvalues ω_n^2, are chosen as positive values. Thus, eqn (34) represents harmonic vibrations, i.e. $f(t) = \exp(\mathrm{i}\omega t)$ and $f_n(t) = \exp(\mathrm{i}\omega_n t)$, respectively, where i is the complex number. Harmonic motion is consistent with the fact that a conservative system has a constant energy. (However, showing mathematically that $\omega_n^2 > 0$ for the boundary conditions discussed above seems possible only for pinned end cases.)

The general solution for eqn (33) is given by

$$\phi_n = \sum_{i=1}^{6} c_i\, \mathrm{e}^{k_{i,n}x}, \tag{35}$$

where c_i = integration constants, which are determined by the boundary conditions, and $k_{i,n}$ are the roots of the following polynomial:

$$(k_{i,n}^2)^3 - \alpha^2(k_{i,n}^2)^2 - \omega_n^2\frac{m}{EI_0}k_{i,n}^2 + \omega_n^2\alpha^2\frac{m}{EI_\infty} = 0. \tag{36}$$

Solving the cubic eqn (36) it can be easily shown that $k_{1,n}^2 < 0$, $k_{2,n}^2 > 0$ and $k_{3,n}^2 > 0$, i.e. the roots are given as $\pm ik_{1,n}$, $\pm k_{2,n}$ and $\pm k_{3,n}$. The general solution can then be written as

$$\phi_n = c_1 \sin(k_{1,n}x) + c_2\cos(k_{1,n}x) + c_3\sinh(k_{2,n}x) + c_4\cosh(k_{2,n}x) + c_5\sinh(k_{3,n}x) + c_6\cosh(k_{3,n}x). \tag{37}$$

The boundary conditions needed to determine the constants c_1–c_6 are given by eqns (16), (17) and (32). The boundary conditions for *pinned and clamped ends* are obtained from eqns (16) and (17), respectively, changing $w \to \phi$ and $p = 0$. For a *free end* the expressions are obtained as

$$\frac{d^2\phi}{dx^2} = 0,$$

$$\frac{d^4\phi}{dx^4} - \omega^2 \frac{m}{EI_0}\phi = 0,$$

$$\frac{d^5\phi}{dx^5} - \alpha^2 \frac{d^3\phi}{dx^3} - \omega^2 \frac{m}{EI_0}\frac{d\phi}{dx} = 0. \tag{38a,b,c}$$

It is noted in eqn (38) that the boundary conditions depend on the eigenvalue ω^2. This is due to inertia forces caused by the distributed mass m.

The roots $k_{1,n}^2 < 0$, $k_{2,n}^2 > 0$ and $k_{3,n}^2 > 0$ in eqn (37) are given by eqn (36). The eigenvalues ω_n^2 in this equation, which provide solutions to the problem, are related to the roots $k_{1,n}^2 < 0$. Equation (36) can then be rewritten as

$$\omega_n^2 = \frac{k_{1,n}^6 + \alpha^2 k_{1,n}^4}{\frac{m}{EI_0}k_{1,n}^2 + \frac{m}{EI_\infty}\alpha^2} = \frac{\omega_{n,\infty}^2 \frac{k_{1,n}^4}{k_{1,n,\infty}^4}}{1 + \frac{\frac{EI_\infty}{EI_0} - 1}{1 + \frac{\alpha^2}{k_{1,n}^2}}} = \frac{\omega_{n,0}^2 \frac{EI_\infty}{EI_0}\frac{k_{1,n}^4}{k_{1,n,0}^4}}{1 + \frac{\frac{EI_\infty}{EI_0} - 1}{1 + \frac{\alpha^2}{k_{1,n}^2}}}, \tag{39}$$

where

$$\omega_{n,0}^2 = \frac{k_{1,n,0}^4 EI_0}{m} \text{ (non-composite action)}, \tag{40}$$

$$\omega_{n,\infty}^2 = \frac{k_{1,n,\infty}^4 EI_\infty}{m} \text{ (full composite action)}. \tag{41}$$

In the general case of arbitrary boundary conditions the eigenvalues are obtained from large and complicated transcendental equations, which require numerical solutions. The iteration is conveniently carried out in the following way:

(1) assume ω_n;
(2) calculate $k_{1,n}$, $k_{2,n}$ and $k_{3,n}$ from eqn (36);
(3) satisfy the transcendental equation.

Once an eigenvalue for a particular set of boundary conditions is known, its associated eigenmode can be determined. This is done by removing one of the equations for the boundary conditions. This leaves five equations in six unknowns which may be solved by assuming the value of one of the c_is.

The non-dimensional fundamental eigenvalues $\omega_1^2/\omega_{1,\infty}^2$ for the four Euler boundary conditions (clamped-free, pinned-pinned, clamped-pinned, clamped-clamped) have been calculated and are shown in Figs 6(a)–6(d) as a function of the non-dimensional parameters $\alpha^2/k_{1,1,\infty}^2$ and EI_∞/EI_0 (solid lines). Note that the first parameter is proportional to the slip modulus K and therefore expresses the degree of composite action. Thus, for $\alpha^2/k_{1,1,\infty}^2 \to 0$ then $\omega_1^2/\omega_{1,\infty}^2 \to \omega_{1,0}^2/\omega_{1,\infty}^2 = EI_0/EI_\infty$ and for $\alpha^2/k_{1,1,\infty}^2 \to \infty$ then $\omega_1^2/\omega_{1,\infty}^2 \to \omega_{1,\infty}^2/\omega_{1,\infty}^2 = 1$.

An approximate solution for composite beams with interlayer slip is here proposed to be obtained by using the characteristic values of $k_{1,n}$ given for beams with full composite action (or non-composite action) as:

$$k_{1,n} \approx k_{1,n,\infty} = k_{1,n,0} = \frac{\pi}{\mu_n L}, \tag{42}$$

where

$$\mu_n = \begin{cases} (n-1/2)^{-1}; & \mu_1 = 1.675 \quad \text{Euler case 1}; \ n \geqslant 2, \\ (n \pm 0)^{-1}; & \mu_1 = 1 \quad \text{Euler case 2}, \\ (n+1/4)^{-1}; & \mu_1 = 0.8 \quad \text{Euler case 3}, \\ (n+1/2)^{-1}; & \mu_1 = 0.667 \quad \text{Euler case 4}, \end{cases} \tag{43a,b,c,d}$$

where Euler case denotes beams with boundary conditions according to the four Euler cases. If eqn (39) is written as

$$\omega_n^2 = \omega_{n,\infty}^2 \frac{EI_{\text{eff}}}{EI_\infty}, \tag{44}$$

where

$$EI_{\text{eff}} = \frac{\dfrac{k_{1,n}^4}{k_{1,n,\infty}^4} EI_\infty}{1 + \dfrac{\dfrac{EI_\infty}{EI_0} - 1}{1 + \dfrac{\alpha^2}{k_{1,n}^2}}}, \tag{45}$$

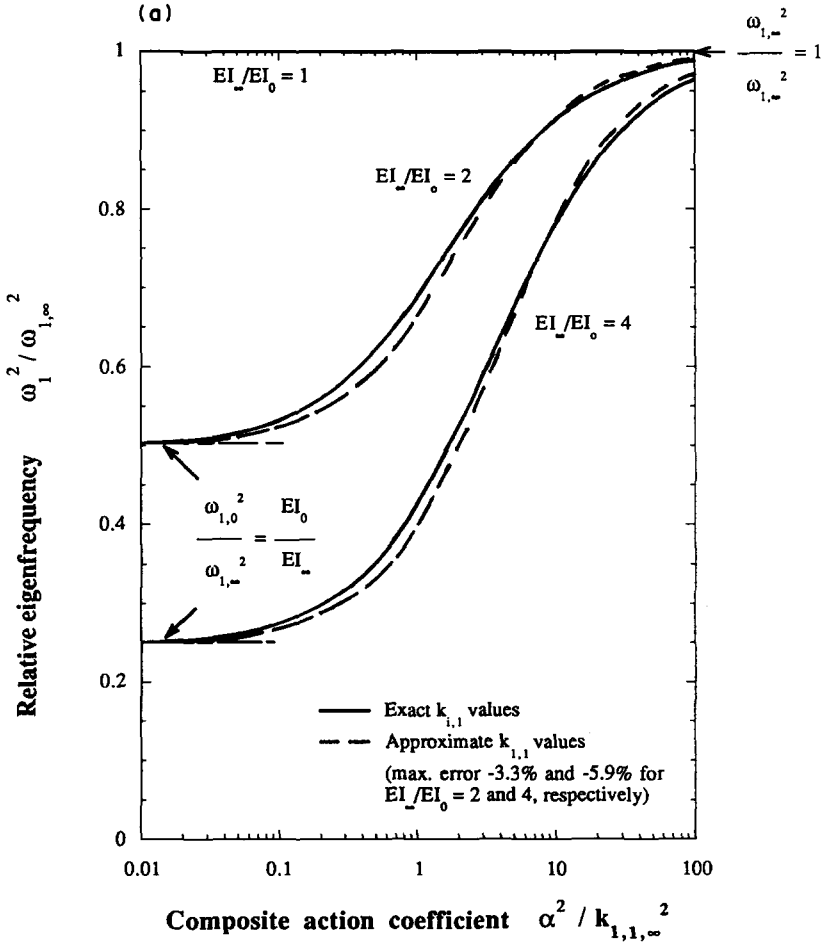

Fig. 6a. Relative eigenfrequency $\omega_1^2/\omega_{1,\infty}^2$ versus $\alpha^2/k_{1,1,\infty}^2$ with different values of EI_∞/EI_0 for Euler case 1 obtained by exact analysis.

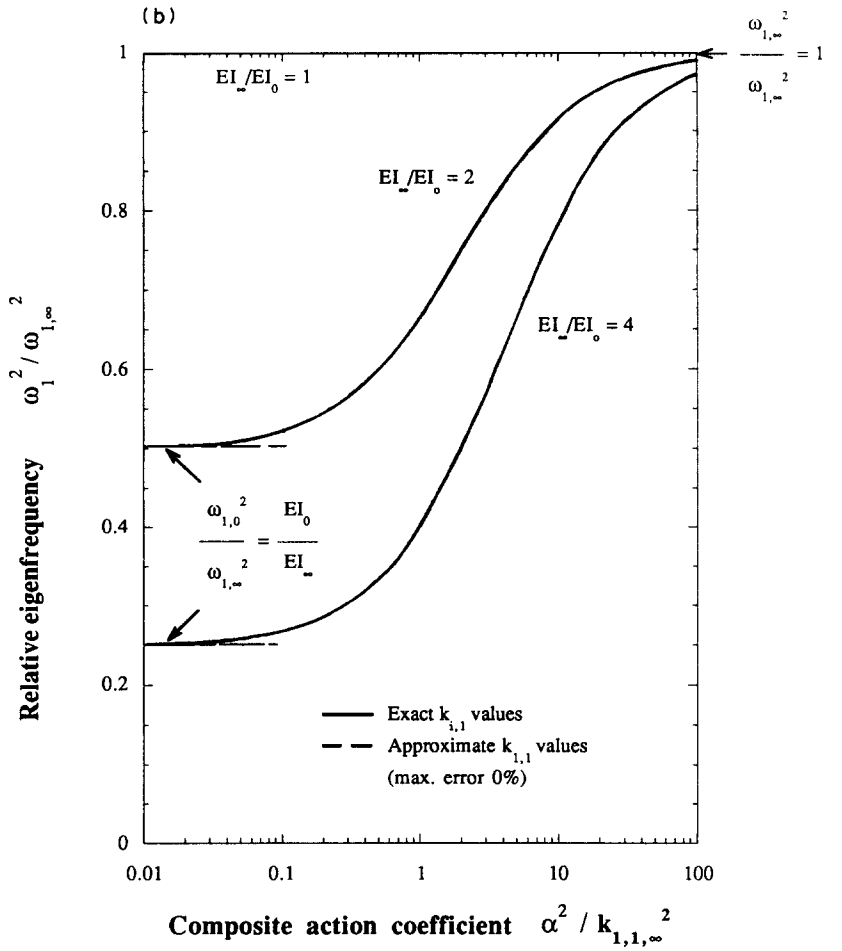

Fig. 6b. Relative eigenfrequency $\omega_1^2/\omega_{1,\infty}^2$ versus $\alpha^2/k_{1,1,\infty}^2$ with different values of EI_∞/EI_0 for Euler case 2 obtained by exact analysis.

the approximate solution (42), i.e. $k_{1,n} \approx k_{1,n,\infty}$, gives

$$EI_{\text{eff}} \approx \frac{EI_\infty}{1 + \dfrac{\dfrac{EI_\infty}{EI_0} - 1}{1 + \dfrac{\alpha^2}{k_{1,n,\infty}^2}}}. \tag{46}$$

EI_{eff} denotes the effective composite bending stiffness for the composite beam with partial interaction [cf. Girhammar (1985b)]. Equation (44) together with (46) is represented in Figs 6(a)–6(b) (dashed lines). (Note that the approximate solution (42), applicable to all n, is compared to the exact solution for $n = 1$.) As is evident from the figures, the accuracy is extremely good for Euler cases 1 and 2 (in fact the exact and approximate values are identical for Euler case 2), but not so good for Euler cases 3 and 4 (maximum error 7–21%). In order to obtain more accurate values for the fundamental eigenfrequency for practical values of the partial composite action parameter $1 < \alpha L < 15$ (which gives $0.28 < \alpha^2/k_{1,1,\infty}^2 < 64$, $0.10 < \alpha^2/k_{1,1,\infty}^2 < 23$, $0.06 < \alpha^2 k_{1,1,\infty}^2 < 15$, and $0.05 < \alpha^2/k_{1,1,\infty}^2 < 10$ for the Euler cases 1, 2, 3 and 4, respectively) the following Euler coefficients should be chosen (a mean value for the two cases $EI_\infty/EI_0 = 2$ and 4 has been chosen):

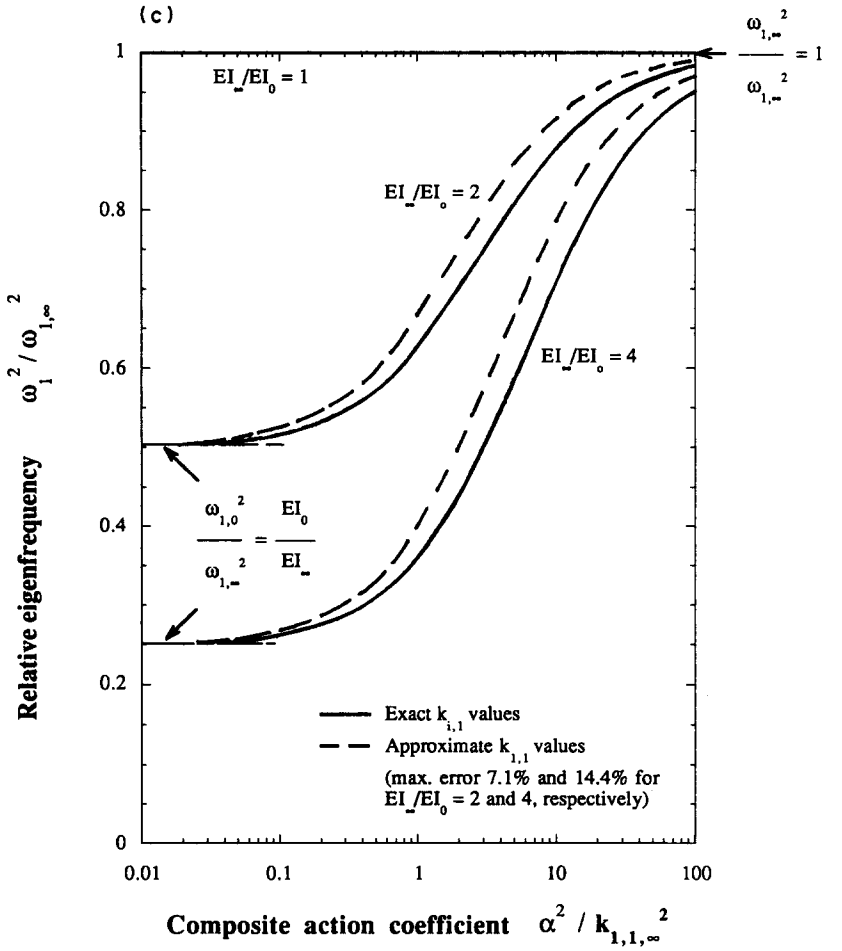

Fig. 6c. Relative eigenfrequency $\omega_1^2/\omega_{1,\infty}^2$ versus $\alpha^2/k_{1,1,\infty}^2$ with different values of EI_∞/EI_0 for Euler case 3 obtained by exact analysis.

$$\mu_1 = \begin{cases} 1.68; & \text{Max. mean error 4\%} \\ 1; & \text{Max. mean error 0\%} \quad \text{for } \dfrac{\alpha^2}{k_{1,1,\infty}^2} > 0.1 \\ 0.82; & \text{Max. mean error 3\%} \\ 0.69; & \text{Max. mean error 5\%} \end{cases} \tag{47a,b,c,d}$$

Knowing the solution ϕ for a given set of boundary conditions, the internal moment can, according to eqn (23), be expressed in terms of the eigenmode as

$$M = e^{i\omega t}\left(\frac{EI_\infty}{\alpha^2}\frac{d^4\phi}{dx^4} - EI_\infty\frac{d^2\phi}{dx^2} - \omega^2\frac{m}{\alpha^2}\frac{EI_\infty}{EI_0}\phi\right). \tag{48}$$

The other internal actions are then obtained from eqns (11)–(15) recognizing that the internal moment now is given by eqn (48) and that $w \to \phi$.

3.3. *Forced vibrations*

Equation (22) is valid only if ϕ_n are an orthogonal set of eigenfunctions satisfying the self-adjoint eigenvalue problem (33) with the homogeneous boundary conditions:

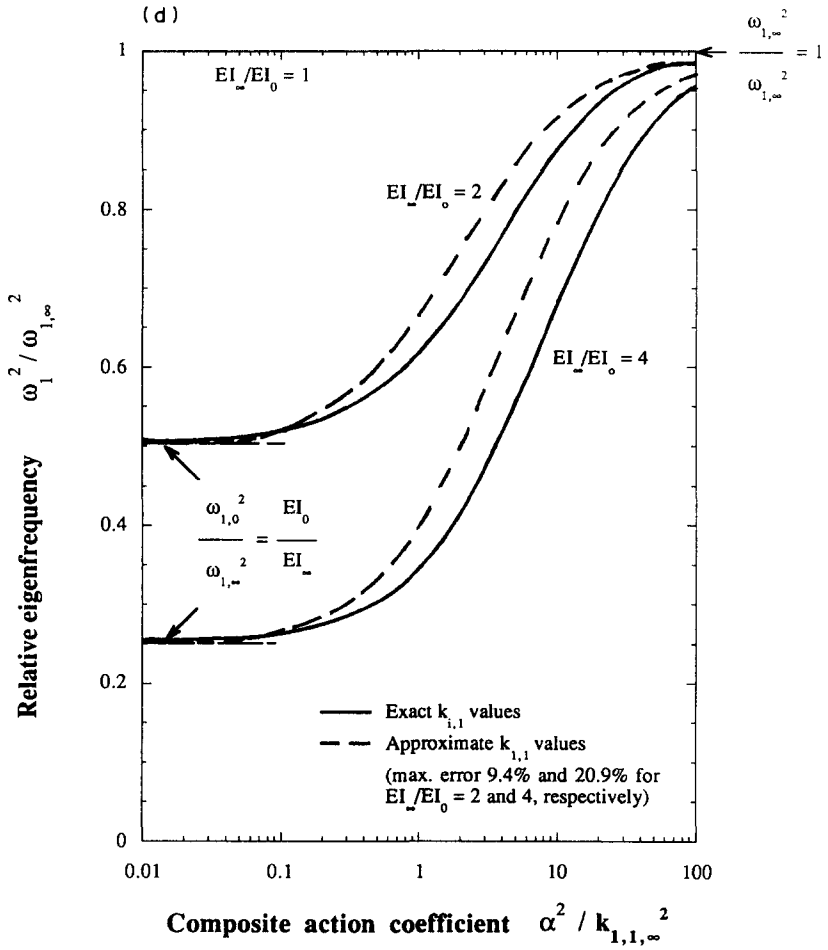

Fig. 6d. Relative eigenfrequency $\omega_i^2/\omega_{i,\infty}^2$ versus $\alpha^2/k_{i,1,\infty}^2$ with different values of EI_∞/EI_0 for Euler case 4 obtained by exact analysis.

$$B_i[\phi] = 0, \tag{49}$$

$$D_j[\phi] = \omega^2 C_j[\phi], \tag{50}$$

and the normalized orthogonality relation,

$$\int_0^L \phi_m \left(\frac{m}{EI_0} \frac{\mathrm{d}^2\phi_n}{\mathrm{d}x^2} - \alpha^2 \frac{m}{EI_\infty} \phi_n \right) \mathrm{d}x + \sum_j \phi_m(0, L) C_j[\phi_n(0, L)] = \delta_{mn}, \tag{51}$$

where $B_i[\phi]$, $D_j[\phi]$, and $C_j[\phi]$ are linear homogeneous differential operators containing derivatives normal to the boundaries $(0, L)$ and along the boundaries $(0, L)$ through order five, and δ_{mn} = Kronecker's delta [cf. Meirovitch (1967)]. The linear homogeneous differential operator C_j in eqn (51) is for *pinned and clamped ends* $C_j = 0$, but $C_1 = m/EI_0$ and $C_2 = (m/EI_0)$ (d/dx) for *free ends* according to eqn (38). (Showing mathematically that the orthogonality relation (51) is fulfilled for the four Euler boundary conditions, seems possible only for pinned and free ends.)

The differential equation for the time function F_n can then be obtained as

$$\frac{d^2F_n}{dt^2} + \omega_n^2 F_n = P_n(t), \tag{52}$$

where

$$P_n(t) = \int_0^L \left(\frac{\alpha^2}{EI_\infty} p - \frac{1}{EI_0}\frac{\partial^2 p}{\partial x^2}\right)\phi_n \, dx. \tag{53}$$

The general solution of eqn (52) is given by Duhamel's integral as

$$F_n = F_n(0)\cos(\omega_n t) + \frac{dF_n(0)}{dt}\frac{\sin(\omega_n t)}{\omega_n} + \frac{1}{\omega_n}\int_0^t P_n(\tau)\sin[\omega_n(t-\tau)]\,d\tau, \tag{54}$$

where $F_n(0)$ and $dF_n(0)/dt$ represent the initial conditions.

3.4. *Application of exact dynamic analysis procedure to simply-supported beams*

The partial composite action theory for forced beam vibrations developed in the preceding section is applied to a simply-supported composite beam subjected to a dynamic uniformly distributed lateral load of constant intensity $p = p_0(t)[\langle x\rangle^0 - \langle x-L\rangle^0]$ (Fig. 7), where $\langle\ \rangle$ denotes Macauley's singularity functions. With the boundary conditions (16) with $w = \phi$ and $p = 0$, the eigenfunctions according to eqn (37) can be written as

$$\phi_n = c_1 \sin(k_{1,n}x); \quad n = 1, 2, 3, \ldots, \tag{55}$$

where

$$k_{1,n} = \frac{n\pi}{L}; \quad n = 1, 2, 3, \ldots, \tag{56}$$

i.e. the same as for a solid beam ($k_{1,n} = k_{1,n,\infty}$). If the eigenfunctions are normalized according to eqn (51), we obtain the integration constant

$$c_1^2 = \frac{1}{\frac{L}{2}\left(\frac{m}{EI_0}k_{1,n}^2 + \alpha^2\frac{m}{EI_\infty}\right)}. \tag{57}$$

The natural frequencies are then given by eqn (44). The time functions are given by eqn (54) where now

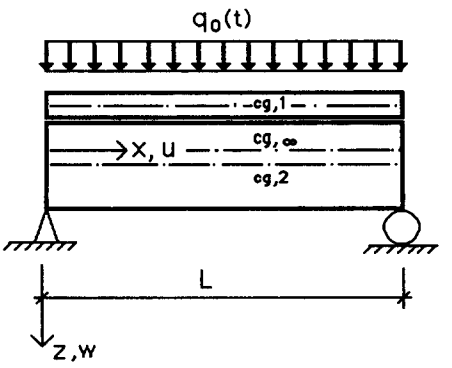

Fig. 7. Simply-supported composite beam subject to dynamic transverse loading.

$$P_n(t) = \frac{p_0(t)\int_0^L \left\{\frac{\alpha^2}{EI_\infty}[\langle x\rangle^0 - \langle x-L\rangle^0] - \frac{1}{EI_0}[\langle x\rangle_{-2} - \langle x-L\rangle_{-2}]\right\}\sin(k_{1,n}x)\,\mathrm{d}x}{\left[\frac{mL}{2}\left(\frac{\alpha^2}{EI_\infty} + \frac{k_{1,n}^2}{EI_\infty}\right)\right]^{1/2}}$$

$$= \frac{p_0(t)\sqrt{2L}}{n\pi\sqrt{m}}\left[\frac{\alpha^2}{EI_\infty} + \frac{k_{1,n}^2}{EI_0}\right]^{1/2}; \quad n = 1, 3, 5, \ldots. \tag{58}$$

The time functions will here be evaluated for two types of dynamic loads: impulsive load and step load.

Impulsive loading. The impulsive loading can be written as:

$$p_0(t) = i_0\langle t\rangle_{-1}, \tag{59}$$

where i_0 = the impulsive loading intensitiy (Ns m^{-1}) and $\langle t\rangle_{-1}$ = Dirac's unit delta function (s^{-1}). The impulsive loading expressed as in eqn (59) includes the condition of initial velocity (Girhammar, 1985a), i.e. the initial conditions are then given as

$$w = \frac{\partial w}{\partial t} = 0 \quad \text{for} \quad t = 0, \tag{60}$$

or

$$F_n(0) = \frac{\mathrm{d}F_n(0)}{\mathrm{d}t} = 0. \tag{61}$$

The time functions are then according to eqns (54) and (58) given by

$$F_n = \frac{i_0\sqrt{2L}}{n\pi\sqrt{m\omega_n}}\left[\frac{\alpha^2}{EI_\infty} + \frac{k_{1,n}^2}{EI_0}\right]^{1/2}\sin(\omega_n t); \quad n = 1, 3, 5, \ldots. \tag{62}$$

The final solution is then given by

$$w = \sum_n \frac{4i_0}{n\pi m\omega_n}\sin\left(\frac{n\pi}{L}x\right)\sin(\omega_n t); \quad n = 1, 3, 5, \ldots. \tag{63}$$

It is noted that the series in eqn (63) is rapidly convergent. The maximum deflection ($x = L/2$) is given by

$$w_{\max} = \sum_n \frac{4i_0\sin\left(\frac{n\pi}{2}\right)}{n\pi m\omega_n}\sin(\omega_n t_{\max}); \quad n = 1, 3, 5, \ldots, \tag{64}$$

where $\omega_n t_{\max}$ is found by solving the equation $\mathrm{d}w_{\max}/\mathrm{d}t = 0$. This must be evaluated numerically (Girhammar and Pan, 1992). Since the first terms in the series above are dominant, a simplified exact theory can be given by using only the first term

$$w_{\max} \approx \frac{4i_0}{\pi m \omega_1}. \tag{65}$$

If, instead of $\omega_n t_{\max}$, $(\omega_n t)_{\max} = n\pi/2$ is used in eqn (64), an upper limit of $w_{\max}$ can be given as

$$w_{\max} \leqslant \sum_n \frac{4i_0 \sin\left(\frac{n\pi}{2}\right)}{n\pi m \omega_n} \sin\left[(\omega_n t)_{\max}\right] = \sum_n \frac{4i_0}{n\pi m \omega_n}; \quad n = 1, 3, 5, \ldots. \tag{66}$$

The corresponding limit cases $\omega_{\max,0}$ and $\omega_{\max,\infty}$ can be obtained from eqns (63)–(66) by substituting ω_n with $\omega_{n,0}$ and $\omega_{n,\infty}$, respectively. The characteristic maximum deflection in the midsection is given by

$$\frac{w_{n,\max}}{w_{n,\max,\infty}} = \frac{\omega_{n,\infty}}{\omega_n} = \left(\frac{EI_\infty}{EI_{\text{eff}}}\right)^{1/2} = \left(1 + \frac{EI_\infty/EI_0 - 1}{1 + \alpha^2/k_{1,n,\infty}^2}\right)^{1/2}. \tag{67}$$

The maximum internal actions are given by eqns (12)–(15) and (23):

$$M_{i,\max} = \sum_n \frac{4i_0 n\pi E_i I_i \sin(n\pi/2)}{mL^2 \omega_n} \sin(\omega_n t_{\max}); \quad n = 1, 3, 5, \ldots, \tag{68}$$

$$N_{1,\max} = -\sum_n \frac{4i_0 EI_\infty \sin(n\pi/2)}{n\pi m L^4 \omega_n \alpha^2 r} \left\{(n\pi)^4 + (n\pi)^2\left(1 - \frac{EI_0}{EI_\infty}\right)\alpha^2 L^2 - \frac{mL^4\omega_n^2}{EI_0}\right\} \sin(\omega_n t_{\max});$$
$$n = 1, 3, 5, \ldots, \tag{69}$$

$$V_{s,\max} = \sum_n \frac{4i_0 EI_\infty}{mL^5 \omega_n \alpha^2 r} \left\{(n\pi)^4 + (n\pi)^2\left(1 - \frac{EI_0}{EI_\infty}\right)\alpha^2 L^2 - \frac{mL^4\omega_n^2}{EI_0}\right\} \sin(\omega_n t_{\max});$$
$$n = 1, 3, 5, \ldots, \tag{70}$$

$$V_{i,\max} = \sum_n \frac{4i_0 EI_\infty r_i}{mL^5 \omega_n \alpha^2 r} \left\{(n\pi)^2 \frac{E_i I_i \alpha^2 L^2 r}{EI_\infty r_i} + (n\pi)^4 + (n\pi)^2\left(1 - \frac{EI_0}{EI_\infty}\right)\alpha^2 L^2 - \frac{mL^4\omega_n^2}{EI_0}\right\} \sin(\omega_n t_{\max}); \quad n = 1, 3, 5, \ldots, \tag{71}$$

where $\omega_n t_{\max}$ in the different equations are found in a similar way as the corresponding value in eqn (64). It is noted that the series in eqns (68)–(71) are slowly convergent or even non-convergent. Simplified exact and upper limit values for the internal actions can be obtained in a similar way as for the deflection w.

Step loading. The step loading can be written as:

$$p_0(t) = p_0 \langle t \rangle^0, \tag{72}$$

where p_0 = the step load intensity [N m^{-1}] and $\langle t \rangle^0$ = Heaviside unit step function [1]. The initial conditions are given by eqns (60) and (61). The time functions are given by:

$$F_n = \frac{p_0\sqrt{2L}}{n\pi\sqrt{m\omega_n^2}}\left[\left(\frac{\alpha^2}{EI_\infty}+\frac{k_{1,n}^2}{EI_0}\right)\right]^{1/2}[1-\cos(\omega_n t)]; \quad n = 1,3,5,\ldots. \tag{73}$$

The final solution is then given by

$$w = \sum_n \frac{4p_0}{n\pi m\omega_n^2}\sin\left(\frac{n\pi}{L}x\right)[1-\cos(\omega_n t)]; \quad n = 1,3,5,\ldots. \tag{74}$$

The convergence of the series in eqn (74) is one degree higher than for the impulsive loading case. The maximum deflection ($x = L/2$) is given by

$$w_{\max} = \sum_n \frac{4p_0\sin(n\pi/2)}{n\pi m\omega_n^2}[1-\cos(\omega_n t_{\max})]; \quad n = 1,3,5,\ldots, \tag{75}$$

where $\omega_n t_{\max}$ is found from the equation $dw_{\max}/dt = 0$. This must be evaluated numerically (Girhammar and Pan, 1992). Using only the first term in the series we obtain

$$w_{\max} \approx \frac{8p_0}{\pi m\omega_1^2}. \tag{76}$$

In the step loading case, no upper limit values similar to those for the impulsive loading are available. The corresponding limit cases $w_{\max,0}$ and $w_{\max,\infty}$ can be obtained in a similar way as for the impulsive loading case. The characteristic maximum deflection in the mid-section is given by

$$\frac{w_{n,\max}}{w_{n,max,\infty}} = \frac{\omega_{n,\infty}^2}{\omega_n^2} = \frac{EI_\infty}{EI_{\text{eff}}} = 1+\frac{EI_\infty/EI_0-1}{1+\alpha^2/k_{1,n,\infty}^2}. \tag{77}$$

The maximum internal actions are given by

$$M_{i,\max} = \sum_n \frac{4p_0 n\pi E_i I_i \sin\left(\frac{n\pi}{2}\right)}{mL^2\omega_n^2}[1-\cos(\omega_n t_{\max})]; \quad n = 1,3,5,\ldots, \tag{78}$$

$$N_{1,\max} = -\sum_n \frac{4p_0 EI_\infty \sin\left(\frac{n\pi}{2}\right)}{n\pi mL^4\omega_n^2\alpha^2 r}\left\{\left[(n\pi)^4+(n\pi)^2\left(1-\frac{EI_0}{EI_\infty}\right)\alpha^2L^2\right][1-\cos(\omega_n t_{\max})]\right.$$
$$\left.+\frac{m\omega_n^2}{EI_0}\cos(\omega_n t_{\max})\right\}+\frac{EI_\infty}{\alpha^2 rEI_0}p_0; \quad n = 1,3,5,\ldots, \tag{79}$$

$$V_{s,\max} = \sum_n \frac{4p_0 EI_\infty}{mL^5\omega_n^2\alpha^2 r}\left\{(n\pi)^2\left[(n\pi)^2+\left(1-\frac{EI_0}{EI_\infty}\right)\alpha^2L^2\right][1-\cos(\omega_n t_{\max})]\right.$$
$$\left.+\frac{m\omega_n^2}{EI_0}\cos(\omega_n t_{\max})\right\}; \quad n = 1,3,5,\ldots, \tag{80}$$

$$V_{i,\max} = \sum_n \frac{4p_0 EI_\infty r_i}{mL^5\omega_n^2\alpha^2 r}\left\{(n\pi)^2\left[\frac{E_i I_i\alpha^2L^2 r}{EI_\infty r_i}+(n\pi)^2+\left(1-\frac{EI_0}{EI_\infty}\right)\alpha^2L^2\right][1-\cos(\omega_n t_{\max})]\right.$$
$$\left.+\frac{m\omega_n^2}{EI_0}\cos(\omega_n t_{\max})\right\}; \quad n = 1,3,5,\ldots. \tag{81}$$

4. APPROXIMATE DYNAMIC ANALYSIS

4.1. *Equivalent single-degree of freedom system*

The rigorous analytical procedures developed in the preceding section are very complex for all but the most simple support and loading conditions and not well suited for design applications. For this reason approximate procedures for determining the deflection, and the internal actions, which correspond to the exact analysis results, are presented here. A comparison of the results obtained from the exact and approximate procedures applied to simply-supported members will be made later in this section.

It is frequently possible to reduce the actual dynamic system to an equivalent system with single-degree of freedom (Biggs, 1964). In order to define an equivalent single-degree system, it is necessary to evaluate the parameters of that system, namely M_e, k_e and P_e, i.e. the equivalent mass (kg), the equivalent stiffness or resistance (N m^{-1}), and the equivalent load (N). The equivalent system is usually selected so that the deflection of the concentrated mass is the same as that for some significant point on the structure, e.g. the midspan of a beam. It should be noted that stresses and forces in the idealized system are not directly equivalent to the same quantities in the structures. However, knowing the deflection, the stresses in the real structure may be readily computed. Since the time scale is not altered, the response of the equivalent system, defined in terms of displacement and time, is exactly the same as that of the significant point on the structure (Biggs, 1964).

The transformation factors for the equivalent system are evaluated on the basis of an assumed shape of the actual structure, usually either the fundamental mode or the static deflection curve. For the methods presented here, the shape will be taken to be the same as that resulting from the static application of the dynamic loads. This approach is considered to be somewhat more accurate, particularly with regard to stress computation, and more general since the characteristic shape is not required (Biggs, 1964). The static deflection curve resulting from static application of the dynamic loads can then be written as:

$$w(x) = w_S \varphi(x), \tag{82}$$

where w_S = static deflection of the significant point on the member, and $\varphi(x)$ = assumed shape of the beam.

The equivalent single degree of freedom system is one for which the kinetic energy, internal strain energy, and work done by all external forces are at all times equal to the same quantities for the complete system with infinite number of degrees of freedom when vibrating in this normal mode alone. Equating kinetic energies:

$$\tfrac{1}{2}M_e\left[\frac{\mathrm{d}w_S(t)}{\mathrm{d}t}\right]^2 = \frac{1}{2}\int_0^L m(x)\left[\frac{\mathrm{d}w_S(t)}{\mathrm{d}t}\varphi(x)\right]^2 \mathrm{d}x, \tag{83}$$

where $w(x,t) = w_S(t)\varphi(x)$, i.e. $w_S(t)$ is now the dynamic deflection of the significant point on the member, and therefore,

$$v_m = \frac{M_e}{M_r} = \frac{\displaystyle\int_0^L m(x)\varphi^2(x)\,\mathrm{d}x}{\displaystyle\int_0^L m(x)\,\mathrm{d}x}, \tag{84}$$

where v_m = transformation factor for the mass and M_r = total real mass of the member. Equating external load energies,

$$P_e(t)w_S(t) = \int_0^L p(x,t)w_S(t)\varphi(x)\,dx, \tag{85}$$

and therefore

$$v_p = \frac{P_e(t)}{P_r(t)} = \frac{\int_0^L p(x,t)\varphi(x)\,dx}{\int_0^L p(x,t)\,dt}, \tag{86}$$

where v_p = transformation factor for the load and $P_r(t)$ = total real load on the member. Equating strain energies:

$$\tfrac{1}{2}k_e w_S^2(t) = \frac{1}{2}\int_0^L \left\{EI_0\left[w_S(t)\frac{d^2\varphi(x)}{dx^2}\right]^2 + \frac{EA_0}{EA_p}N_1^2 + \frac{V_s^2}{K}\right\}dx, \tag{87}$$

where N_1 and V_s are given by the expressions in the dynamic case corresponding to eqns (12) and (13), respectively, in terms of $w(x,t) = w_S(t)\varphi(x)$. The terms on the right-hand side refer to the strain energy due to the internal moments, the strain energy due to the internal axial forces and the slip energy due to the interlayer shear force, respectively. Instead of solving the rather complicated integral (87), the following reasoning can be applied to evaluate the integral in an alternative way. The stiffness of a beam is the internal force tending to restore the member to its unloaded position. If we define this resistance in terms of the load distribution for which the analysis is being made, the stiffness is numerically equal to the total load of the same distribution which would cause a unit deflection at the point where the deflection is equal to that of the equivalent system (Biggs, 1964). Thus, the transformation factor for the stiffness (v_k) must be equal to the load factor, i.e.

$$v_k = v_p. \tag{88}$$

The assumed shape of the actual beam is thus given by eqns (8) and (9).

The equation of motion for the equivalent single degree of freedom system is given by

$$M_e\frac{d^2w_S(t)}{dt^2} + k_e w_S(t) = P_e(t) \tag{89}$$

or

$$v_m M_r\frac{d^2w_S(t)}{dt^2} + v_k k_r w_S(t) = v_p P_r(t), \tag{90}$$

where k_r = stiffness or resistance of the real member subject to the total real load distribution considered as a static load, i.e. $p(x)$. The general solution is

$$w_S = w_S(0)\cos(\omega_e t) + \frac{dw_S(0)}{dt}\frac{\sin(\omega_e t)}{\omega_e} + \frac{1}{\omega_e M_e}\int_0^t P_e(\tau)\sin[\omega_e(t-\tau)]\,d\tau, \tag{91}$$

where

$$\omega_e^2 = \frac{k_e}{M_e} = \frac{\nu_k k_r}{\nu_m M_r}. \tag{92}$$

4.2. *Application of approximate dynamic analysis procedure to simply-supported beams*

The equivalent single degree of freedom system method for layered beam vibrations developed in the preceding section is applied to the simply-supported beam discussed before (Fig. 7). The static deflection curve is, according to Girhammar and Gopu (1993a), given by

$$w(x) = \frac{p_0 L^4}{24 EI_\infty}\left\{\left[\left(\frac{x}{L}\right)^4 - 2\left(\frac{x}{L}\right)^3 + \frac{x}{L}\right] + \frac{24}{\alpha^4 L^4}\left(\frac{EI_\infty}{EI_0} - 1\right)\left[\cosh(\alpha x) - \tanh\left(\frac{\alpha L}{2}\right)\sinh(\alpha x) + \tfrac{1}{2}\alpha^2 x^2 + \tfrac{1}{2}\alpha^2 x L - 1\right]\right\}, \tag{93}$$

i.e.

$$w_S = \frac{p_0 L^4}{24 EI_\infty}\left\{\frac{5}{16} + \frac{24}{\alpha^4 L^4}\left(\frac{EI_\infty}{EI_0} - 1\right)\left[\frac{1}{\cosh(\alpha L/2)} + \frac{\alpha^2 L^2}{8} - 1\right]\right\}, \tag{94}$$

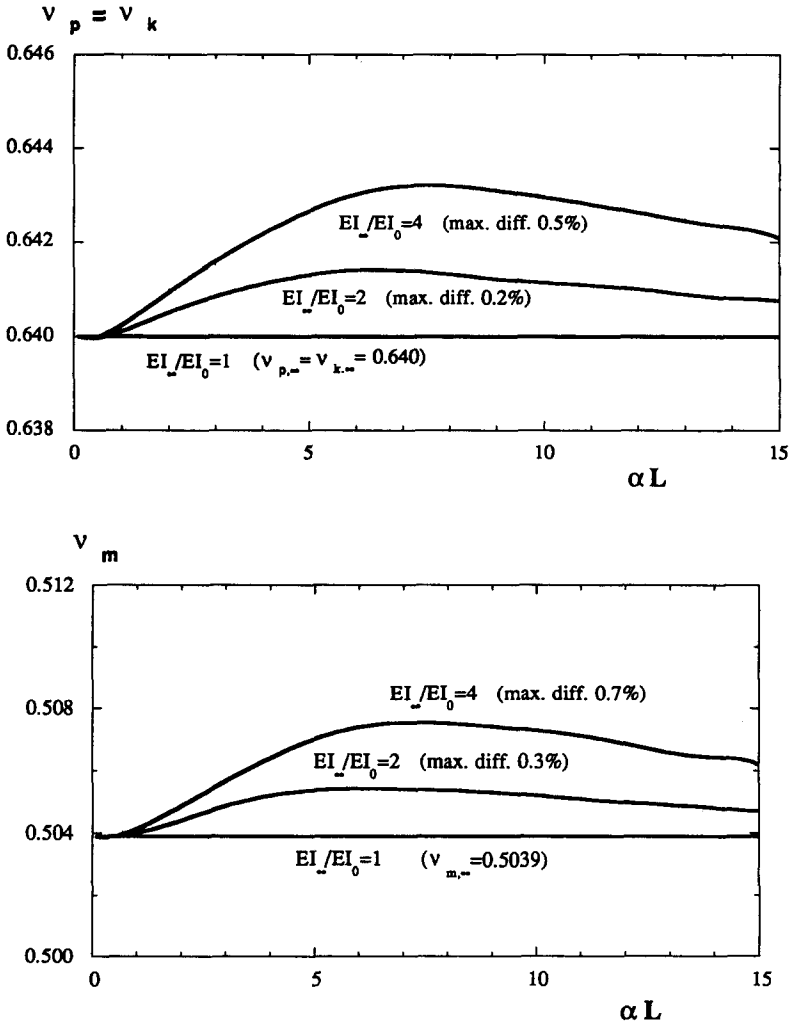

Fig. 8. Transformation factors for uniformly loaded simply-supported composite beams versus αL and EI_∞/EI_0.

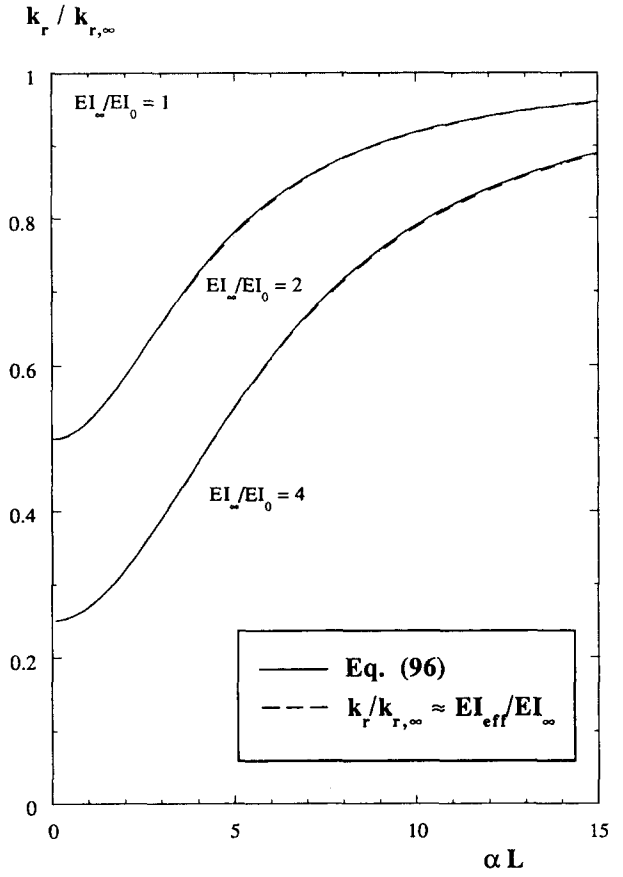

Fig. 9. Relative stiffness $k_r/k_{r,\infty}$ versus αL and EI_∞/EI_0.

$$\varphi(x) = \frac{\left(\frac{x}{L}\right)^4 - 2\left(\frac{x}{L}\right)^3 + \frac{x}{L} + \frac{24}{\alpha^4 L^4}\left(\frac{EI_\infty}{EI_0} - 1\right) \times \left[\cosh(\alpha x) - \tanh\left(\frac{\alpha L}{2}\right)\sinh(\alpha x) - \tfrac{1}{2}\alpha^2 x^2 + \tfrac{1}{2}\alpha^2 x L - 1\right]}{\frac{5}{16} + \frac{24}{\alpha^4 L^4}\left(\frac{EI_\infty}{EI_0} - 1\right)\left[\frac{1}{\cosh(\alpha L/2)} + \frac{\alpha^2 L^2}{8} - 1\right]}. \tag{95}$$

Then the transformation factors can be calculated according to eqns (84), (86) and (88). The factors are shown in Fig. 8 as a function of αL and EI_∞/EI_0. For a fully composite section ($\alpha L \to \infty$), the transformation factors are $v_{m,\infty} = 0.504$ and $v_{p,\infty} = v_{k,\infty} = 0.640$. It is evident from the figures that the same transformation factors as for solid members can also be used for simply-supported composite beams with interlayer slip. The equivalent parameters are then given by $M_e = v_m mL$, $P_e(t) = v_p p_0(t)L$, $k_e = v_k k_r$, $\omega_e^2 = k_e/M_e$, where

$$k_r = \frac{k_{r,\infty}}{1 + \frac{384}{5\alpha^4 L^4}\left(\frac{EI_\infty}{EI_0} - 1\right)\left[\frac{1}{\cosh(\alpha L/2)} + \frac{\alpha^2 L^2}{8} - 1\right]}, \tag{96}$$

where the stiffness for a beam with full composite action is $k_{r,\infty} = 384EI_\infty/5L^3$. The relative stiffness of the composite beam according to eqn (96) is shown in Fig. 9 versus αL and EI_∞/EI_0 (solid lines). Equation (96) is also compared to the approximate stiffness using the effective bending stiffness according to eqn (46) for the fundamental mode ($n = 1$), i.e.

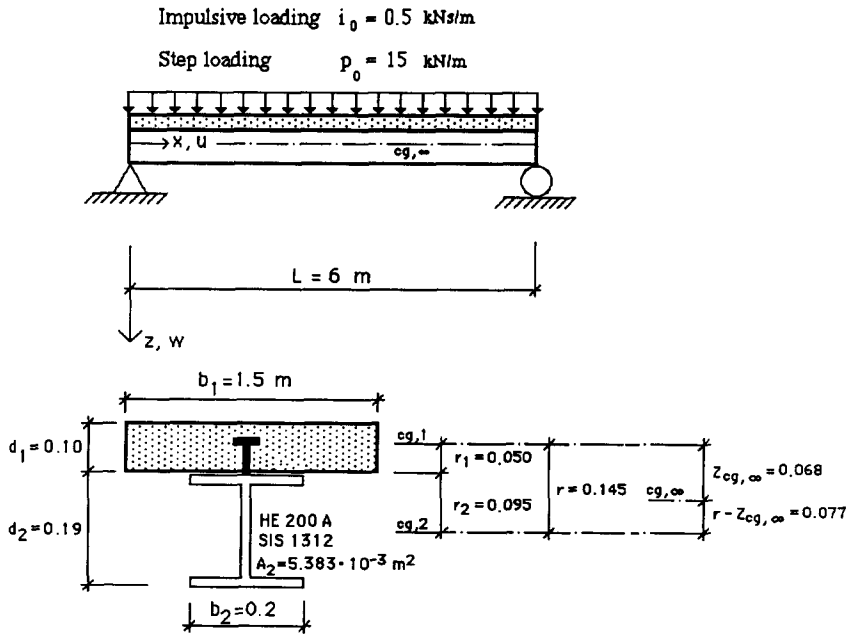

m_1 = 360.0 kg/m	m_2 = 42.4 kg/m	m = 402.4 kg/m
E_1A_1 = 1275.0 MN	E_2A_2 = 1129.8 MN	EA_0 = 2404.8 MN
E_1I_1 = 1.063 MNm²	E_2I_2 = 7.749 MNm²	EI_0 = 8.812 MNm²
$\beta r/\alpha^2$ = 0.588	γ/α^2 = 0.530	EI_∞ = 21.388 MNm²
K = 400 MPa	αL = 7.644	

Fig. 10. Simply-supported composite beam of concrete and steel subject to impulsive and step loading, respectively.

$k_{r,\infty} \approx 384EI_{\text{eff}}/5L^3$ for $k_{1,1,\infty} = \pi/\text{L}$ (dashed lines). It is evident from the figures that the effective bending stiffness is very close to the exact one. This effective bending stiffness developed for a vibrating composite beam is for a simply-supported beam the same as the effective bending stiffness developed earlier for buckling of a composite beam-column (Girhammar and Gopu, 1993a). Since the stiffness k_r is evaluated under static conditions, the latter effective bending stiffness should be used for the general case.

The deflection in the significant point on the beam (midspan) will be evaluated here for the same types of dynamic loads as before.

Impulsive loading. Using eqns (59) and (60) in eqn (91) we get

$$w_{\text{S}}(t) = \frac{v_p i_0 L}{\omega_e M_e} \sin(\omega_e t). \tag{97}$$

The corresponding limit cases $w_{\text{S},0}(t)$ and $w_{\text{S},\infty}(t)$ can be obtained by substituting ω_e, v_p and M_e with their values in the non-composite and full composite action cases, respectively. The relative amplitude of the midspan deflection is then given by $w_{\text{S}}/w_{\text{S},\infty} \approx (k_{r,\infty}/k)^{1/2} \approx (EI_\infty/EI_{\text{eff}})^{1/2}$ (since $v_k = v_p \approx v_{k,\infty} = v_{p,\infty}$ and $v_m \approx v_{m,\infty}$). The maximum internal actions are obtained by using eqns (97), (95) and (82) in eqns (12)–(15), i.e.

$$M_{i,\max} = \frac{v_p i_0 E_i I_i}{C\omega_e M_e L}\left\{3 + \frac{24}{\alpha^2 L^2}\left(\frac{EI_\infty}{EI_0} - 1\right)\frac{\cosh(\alpha L/2) - 1}{\cosh(\alpha L/2)}\right\}\sin(\omega_e t), \tag{98}$$

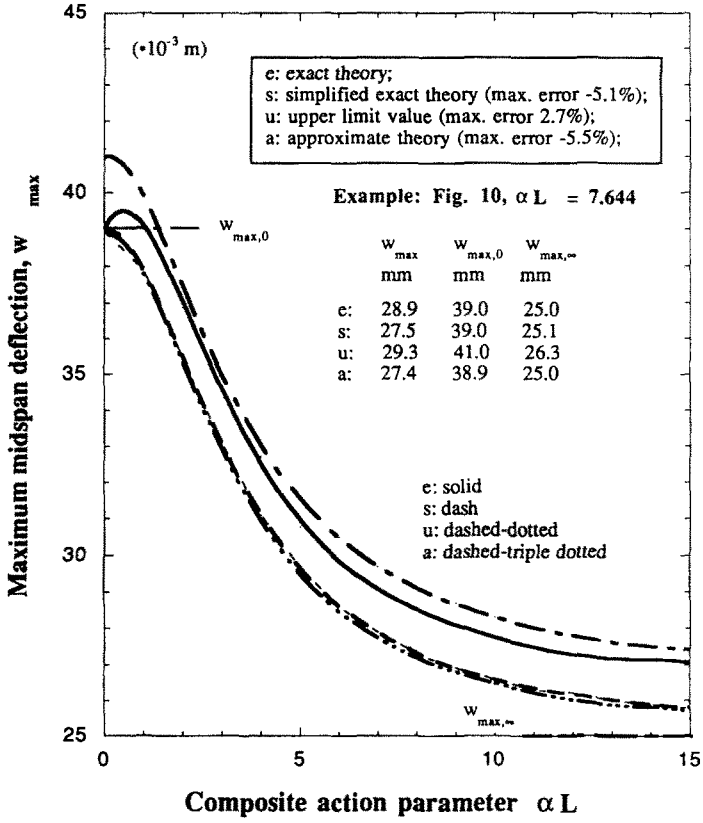

Fig. 11. Maximum midspan deflection of simply-supported concrete–steel beam obtained from the exact and approximate theories versus αL under impulsive loading.

$$N_{1,\max} = -\frac{v_p i_0 EI_\infty}{C\omega_e M_e Lr}\left\{\frac{24}{\alpha^2 L^2}\left[1+\left(\frac{EI_\infty}{EI_0}-1\right)\frac{1}{\cosh(\alpha L/2)}\right]\right.$$
$$\left.+\left(1-\frac{EI_0}{EI_\infty}\right)\left[3+\frac{24}{\alpha^2 L^2}\left(\frac{EI_\infty}{EI_0}-1\right)\frac{\cosh(\alpha L/2)-1}{\cosh(\alpha L/2)}\right]-\frac{CmL^2\omega_e^2}{\alpha^2 EI_0}\right\}\sin(\omega_e t), \quad (99)$$

$$V_{s,\max} = \frac{v_p i_0 EI_\infty}{C\omega_e M_e L^2 r}\left\{-\frac{24}{\alpha L}\left(\frac{EI_\infty}{EI_0}-1\right)\tanh(\alpha L/2)+\left(1-\frac{EI_0}{EI_\infty}\right)\right.$$
$$\times\left[12+\frac{24}{\alpha L}\left(\frac{EI_\infty}{EI_0}-1\right)\tanh(\alpha L/2)\right]-\frac{mL^2\omega_e^2}{\alpha^2 EI_0}\left[1-\frac{24}{\alpha^3 L^3}\left(\frac{EI_\infty}{EI_0}-1\right)\right.$$
$$\left.\left.\times\left[\tanh(\alpha L/2)-\tfrac{1}{2}\alpha L\right]\right]\right\}\sin(\omega_e t), \quad (100)$$

$$V_{i,\max} = \frac{v_p i_0 EI_\infty r_i}{C\omega_e M_e L^2 r}\left\{\frac{12E_iI_ir}{EI_\infty r_i}+\frac{24}{\alpha L}\left(\frac{E_iI_ir}{EI_\infty r_i}-1\right)\left(\frac{EI_\infty}{EI_0}-1\right)\tanh(\alpha L/2)\right.$$
$$+\left(1-\frac{EI_0}{EI_\infty}\right)\left[1+\frac{24}{\alpha L}\left(\frac{EI_\infty}{EI_0}-1\right)\tanh(\alpha L/2)\right]-\frac{mL^2\omega_e^2}{\alpha^2 EI_0}$$
$$\left.\times\left[1-\frac{24}{\alpha^3 L^3}\left(\frac{EI_\infty}{EI_0}-1\right)\left[\tanh(\alpha L/2)-\tfrac{1}{2}\alpha L\right]\right]\right\}\sin(\omega_e t), \quad (101)$$

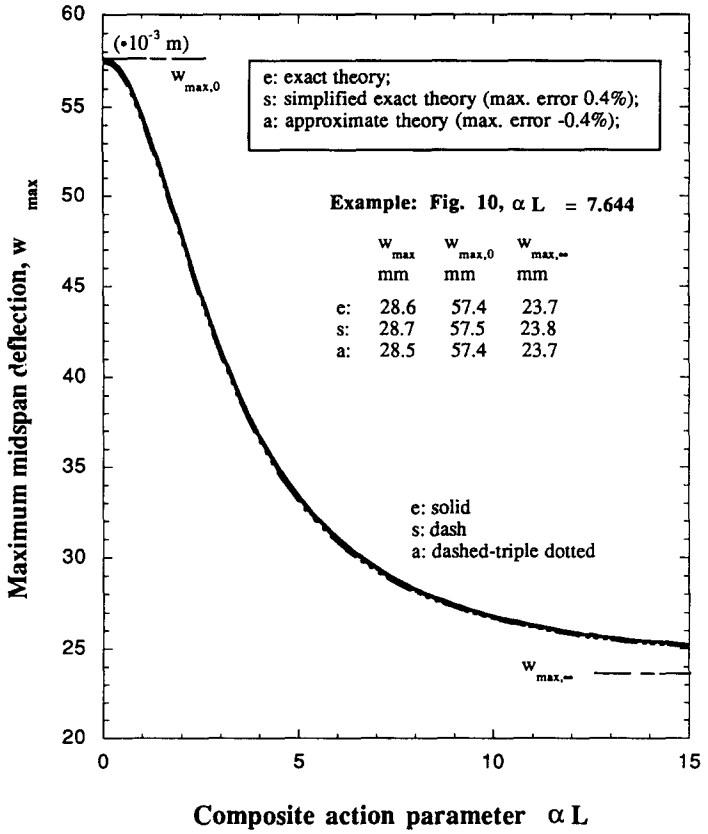

Fig. 12. Maximum midspan deflection of simply-supported concrete–steel beam obtained from the exact and approximate theories versus αL under step loading.

where

$$C = \frac{5}{16} + \frac{24}{\alpha^4 L^4}\left(\frac{EI_\infty}{EI_0} - 1\right)\left[\frac{1}{\cosh(\alpha L/2)} + \frac{\alpha^2 L^2}{8} - 1\right]. \tag{102}$$

Step loading. Using eqns (72) and (60) in eqn (91) we get

$$w_S(t) = \frac{\nu_p p_0 L}{\omega_e^2 M_e}[1 - \cos(\omega_e t)]. \tag{103}$$

The corresponding limit cases $w_{S,0}(t)$ and $w_{S,\infty}(t)$ can be obtained by substituting ω_e, ν_p and M_e with their values in the non-composite and full composite action cases, respectively. The relative amplitude of the midspan deflection is then given by $w_S/w_{S,\infty} \approx k_\infty/k \approx EI_\infty/EI_{\text{eff}}$ (since $\nu_k = \nu_p \approx \nu_{k,\infty} = \nu_{p,\infty}$ and $\nu_m \approx \nu_{m,\infty}$). The maximum internal actions are obtained by using eqns (103), (95) and (82) in eqns (12)–(15), i.e.

$$M_{i,\max} = \frac{\nu_p p_0 E_i I_i}{C\omega_e^2 M_e L}\left\{3 + \frac{24}{\alpha^2 L^2}\left(\frac{EI_\infty}{EI_0} - 1\right)\frac{\cosh(\alpha L/2) - 1}{\cosh(\alpha L/2)}\right\}[1 - \cos(\omega_e t)], \tag{104}$$

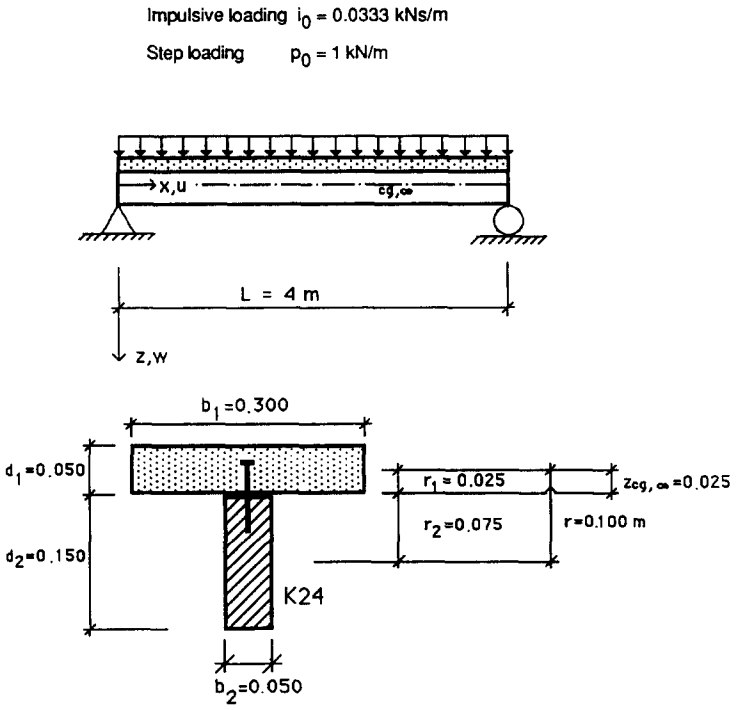

m_1 = 36.0 kg/m	m_2 = 3.75 kg/m	m = 39.75 kg/m
E_1A_1 = 180.0 MN	E_2A_2 = 60 MN	EA_0 = 240 MN
E_1I_1 = 0.0375 MNm^2	E_2I_2 = 0.1125 MNm^2	EI_0 = 0.150 MNm^2
$\beta r/\alpha^2$ = 0.75	γ/α^2 = 0.75	EI_∞ = 4EI0 = 0.60 MNm^2
K = 50 MPa	αL = 8.433	

Fig. 13. Simply-supported composite beam of concrete and wood subject to impulsive and step loading, respectively.

$$N_{1,\max} = -\frac{v_p p_0 EI_\infty}{C\omega_e^2 M_e L r}\left\{\frac{24}{\alpha^2 L^2}\left[1+\left(\frac{EI_\infty}{EI_0}-1\right)\frac{1}{\cosh(\alpha L/2)}\right]\right.$$

$$\left.+\left(1-\frac{EI_0}{EI_\infty}\right)\left[3+\frac{24}{\alpha^2 L^2}\left(\frac{EI_\infty}{EI_0}-1\right)\frac{\cosh(\alpha L/2)-1}{\cosh(\alpha L/2)}\right]\right\}[1-\cos(\omega_e t)]$$

$$-\frac{v_p p_0 EI_\infty}{M_e L r}\frac{mL^2}{\alpha^2 EI_0}\cos(\omega_e t), \quad (105)$$

$$V_{s,\max} = \frac{v_p p_0 EI_\infty}{C\omega_e^2 M_e L^2 r}\left\{-\frac{24}{\alpha L}\left(\frac{EI_\infty}{EI_0}-1\right)\tanh(\alpha L/2)\right.$$

$$\left.+\left(1-\frac{EI_0}{EI_\infty}\right)\left[12+\frac{24}{\alpha L}\left(\frac{EI_\infty}{EI_0}-1\right)\tanh(\alpha L/2)\right]\right\}[1-\cos(\omega_e t)]$$

$$-\frac{v_p p_0 EI_\infty}{CM_e L^2 r}\frac{mL^2}{\alpha^2 EI_0}\left\{1-\frac{24}{\alpha^3 L^3}\left(\frac{EI_\infty}{EI_0}-1\right)[\tanh(\alpha L/2)-\tfrac{1}{2}\alpha L]\right\}\cos(\omega_e t), \quad (106)$$

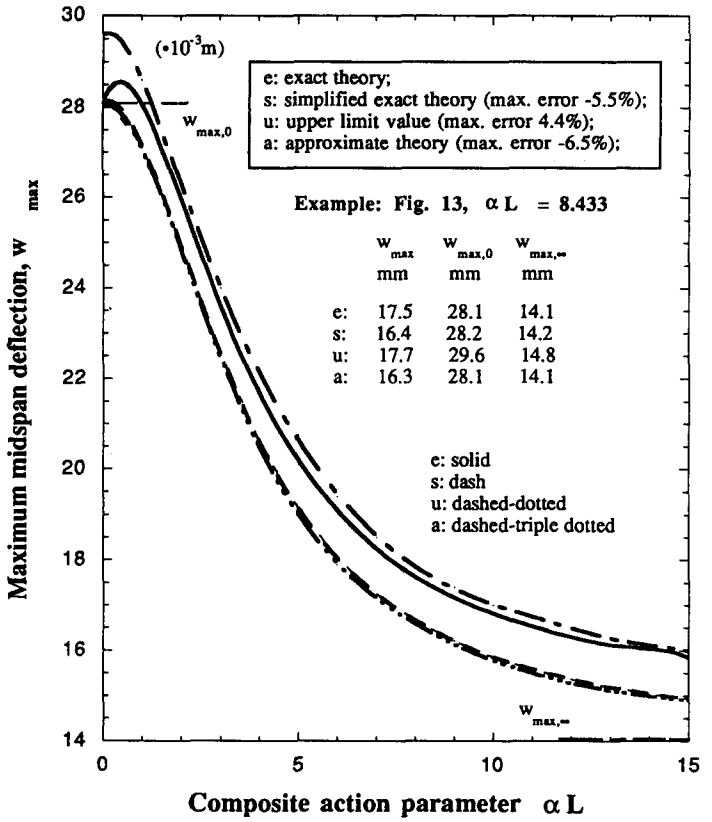

Fig. 14. Maximum midspan deflection of simply-supported concrete–wood beam obtained from the exact and approximate theories versus αL under impulsive loading.

$$V_{i,\max} = +\frac{v_p p_0 E I_\infty r_i}{C\omega_e^2 M_e L^2 r}\left\{\frac{12E_iI_ir}{EI_\infty r_i}+\frac{24}{\alpha L}\left(\frac{E_iI_ir}{EI_\infty r_i}-1\right)\left(\frac{EI_\infty}{EI_0}-1\right)\tanh(\alpha L/2)\right.$$
$$\left.+\left(1-\frac{EI_0}{EI_\infty}\right)\left[12+\frac{24}{\alpha L^4}\left(\frac{EI_\infty}{EI_0}-1\right)\tanh(\alpha L/2)\right]\right\}[1-\cos(\omega_e t)]$$
$$-\frac{v_p p_0 E I_\infty r_i}{C M_e L^2 r}\frac{mL^2}{\alpha^2 EI_0}\left\{1-\frac{24}{\alpha^3 L^3}\left(\frac{EI_\infty}{EI_0}-1\right)[\tanh(\alpha L/2)-\tfrac{1}{2}\alpha L]\right\}\cos(\omega_e t), \quad (107)$$

where C is given by eqn (102).

5. ILLUSTRATIVE EXAMPLES

The deflection and internal actions in the concrete–steel composite beam shown in Fig. 10 and the concrete–wood composite beam in Fig. 13 are computed for different slip modulus values by using the expressions obtained from the exact analysis procedure and from the approximate procedure. The deflections obtained from the two procedures are compared in terms of their maximum values in Figs 11, 12 and Figs 14, 15, respectively, for different values of αL.

The analyses show that the displacements obtained by the approximate theory are extremely close to the exact values for these particular cases. For the case of impulsive loading, the errors are less than 6% and for the case of step loading, the errors are less than 1%.

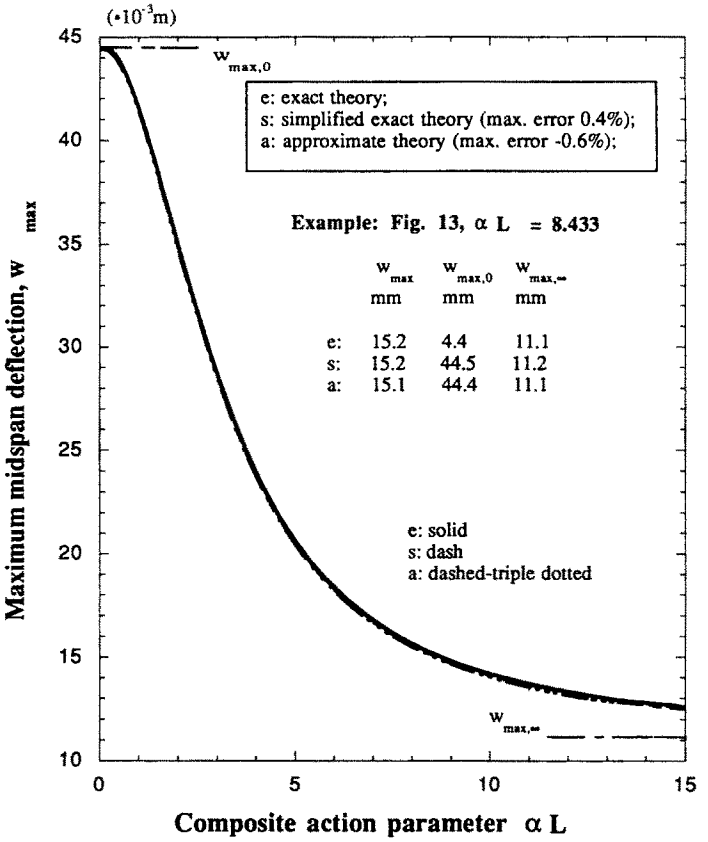

Fig. 15. Maximum midspan deflection of simply-supported concrete–wood beam obtained from the exact and approximate theories versus αL under step loading.

6. SUMMARY

Closed-form solutions for the displacement functions and internal actions in composite members with interlayer slip and various boundary conditions are developed from an exact analysis procedure based on the one-dimensional linear elastic partial composite action theory, and an approximate analysis procedure based on a single degree of freedom equivalent system. The methods proposed are general in nature and can be applied to different loading conditions, material and geometry parameters. The admissable boundary conditions necessary to solve for the eigenfrequencies in the exact analysis case are presented. The validity of the solutions are demonstrated by comparing their solutions at their lower and upper limits with well-known results for ordinary beams with non-composite and full composite sections, respectively. Non-dimensional graphs are generated to show the effects of variation in the physical and geometric properties of the subelements and in the shear connector properties on the eigenfrequencies of composite members with boundary conditions according to the four Euler cases. An approximate solution for the eigenfrequencies in the exact analysis procedure is also proposed and evaluated by comparison with the non-dimensional graphs based on the exact solution. The Euler coefficients to be used in the approximate solution for the fundamental eigenfrequencies of composite members with boundary conditions corresponding to the four Euler cases are presented.

The exact and approximate analysis procedures are applied to a simply-supported beam to illustrate the difference in the two solutions. The transformation factors for uniformly loaded simply-supported composite beams were found to be approximately the same as those for solid beams. The analysis procedures are applied to the following cases: concrete–steel beam under impulsive and step loadings, and concrete–wood beam under impulsive and step loadings. The analyses show that the displacements obtained by the approximate

theory are extremely close to the exact values for these particular cases. For the case of impulsive loading, the errors are less than 6% and for the case of step loading, the errors are less than 1%.

REFERENCES

Biggs, I. M. (1964). *Introduction to Structural Dynamics*. McGraw-Hill, New York.

Girhammar, U. A. (1985a). Dynamic analysis of composite structures of concrete, steel and wood. Royal Swedish Fortifications Administration, Report A5:85, Eskilstuna (in Swedish).

Girhammar, U. A. (1985b). Composite wood structures. *J. Swedish Soc. Civ. Engrs* **3**, 37–42 (in Swedish).

Girhammar, U. A. (1992). Simplified analysis methods for composite members with interlayer slip. Royal Institute of Technology (KTH), Stockholm.

Girhammar, U. A. and Gopu, V. K. A. (1991). Analysis of P-Δ effect in composite concrete/timber beam-columns. *Proc. Inst. Civ. Engrs* **91**, 39–54.

Girhammar, U. A. and Gopu, V. K. A. (1993a). Composite beam-columns with interlayer slip—exact analysis. *J. Struct. Engng, ASCE* (to be published).

Girhammar, U. A. and Gopu, V. K.A. (1993b). Composite beam-columns with interlayer slip—approximate analysis. *J. Struct. Engng, ASCE* (under review).

Girhammar, U. A. and Pan, D. (1992). Free and forced vibrations of composite members with interlayer slip. Royal Institute of Technology (KTH), Stockholm.

Henghold, W. M. (1972). Layered beam vibrations including slip. Colorado State University, Civil Engineering Department, Doctoral Dissertation, Fort Collins.

Meirovitch, L. (1967). *Analytical Methods in Vibrations*. MacMillan, New York.